

GRAS SAF Report 05
Ref: SAF/GRAS/METO/REP/GSR/005
Web: www.grassaf.org
Date: 23 January 2008

The EUMETSAT
Network of
Satellite Application
Facilities



GRAS SAF Report 05

Refractivity calculations in ROPP

Huw Lewis

Met Office, UK

Document Author Table

	Name	Function	Date	Comments
Prepared by:	H. Lewis	GRAS SAF Project Team	23 January 2008	
Reviewed by:	D. Offiler	GRAS SAF Project Team	23 January 2008	
Approved by:	K.B. Lauritsen	GRAS SAF Project Manager	17 October 2008	

Document Change Record

Issue/Revision	Date	By	Description
Version 1.0	23 Jan 2008	HL	First version

GRAS SAF Project

The GRAS SAF is a EUMETSAT-funded project responsible for operational processing of GRAS radio occultation data from the Metop satellites. The GRAS SAF delivers bending angle, refractivity, temperature, pressure, and humidity profiles in near-real time and offline for NWP and climate users. The offline profiles are further processed into climate products consisting of gridded monthly zonal means of bending angle, refractivity, temperature, humidity, and geopotential heights together with error descriptions.

The GRAS SAF also maintains the Radio Occultation Processing Package (ROPP) which contains software modules that will aid users wishing to process, quality-control and assimilate radio occultation data from any radio occultation mission into NWP and other models.

The GRAS SAF Leading Entity is the Danish Meteorological Institute (DMI), with Cooperating Entities: i) European Centre for Medium-Range Weather Forecasts (ECMWF) in Reading, United Kingdom, ii) Institut D'Estudis Espacials de Catalunya (IEEC) in Barcelona, Spain, and iii) Met Office in Exeter, United Kingdom. To get access to our products or to read more about the project please go to <http://www.grassaf.org>.

1 Background

The ROPP forward model aims to calculate profiles of refractivity N from profiles of pressure p , temperature T and humidity q for comparison with the observed refractivity measured during an occultation as part of a data assimilation process. This is achieved in the `ropp_fm_refrac_1d` subroutine. The forward model used to assimilate bending angle is also dependent on first calculating the refractivity profile which is used to derive bending angle using the Abel transform. This is achieved in the `ropp_fm_bangle_1d` subroutine.

A detailed description of the relationship between refractivity and atmospheric properties was provided by (4). At microwave frequencies in the Earth's atmosphere, N varies due to contributions from the dry neutral atmosphere, water vapour, free electrons in the ionosphere and particulates.

$$N = 77.6 \frac{p}{T} + 3.73 \times 10^5 \frac{e}{T^2} + 4.03 \times 10^7 \frac{n_e}{f^2} + 1.4W \quad (1.1)$$

The first term is the dry neutral atmosphere contribution where p is the atmospheric pressure in hPa and T the temperature in Kelvin. The second term is the water vapour contribution where e is the partial water vapour pressure in hPa, which is a function of pressure p and specific humidity q as

$$e = \frac{pq}{\epsilon_w + (1 - \epsilon_w)q} \quad (1.2)$$

where ϵ_w is the ratio of molecular weight of water to that of dry air (0.622). The third ionospheric contribution results from free electrons in the ionosphere where n_e is the electron number density per cubic metre and f is the transmitter frequency in Hz. This term only becomes important above a height of 60-90 km (4). The final term results from scattering by particulates. This is dominated by liquid water droplets and only this contribution is expressed in Equation 1.1 where W is the liquid water vapour content in grams per cubic metre.

Figure 1.1 illustrates the relative contribution of the terms in Equation 1.1 to the refractivity for a sample atmospheric profile. The dry neutral atmosphere term clearly dominates, accounting for about 90% of the computed refractivity within the troposphere, where water vapour contributes 10%, and almost 100% in the stratosphere. The ionospheric term is likely to dominate above about 60 km, the top of the NWP model used in this case. Using a typical value for the electron density n_e at 100 km altitude of 10^{10} m^{-3} (3), gives a value for the third term in Equation 1.1 of 0.16 ($f=1.5 \text{ GHz}$), several times greater than the dry neutral atmosphere term of about 0.01. In any case, the ionospheric contribution to refractivity can be isolated and removed from the refractivity observations by using information measured at two GPS transmitter frequencies (4). The final term in Equation 1.1 can be estimated using typical values for the liquid water content of between 0.2 gm^{-3} (293 K) and 0.04 gm^{-3} (253 K) (2). This gives contributions to the refractivity of between 0.28 and 0.06, which is small in comparison with the other neutral atmosphere terms over most of the region of interest.

For refractivity calculations in the troposphere and stratosphere, as required for assimilation of GPSRO data into NWP for example, the following two-term approximation can

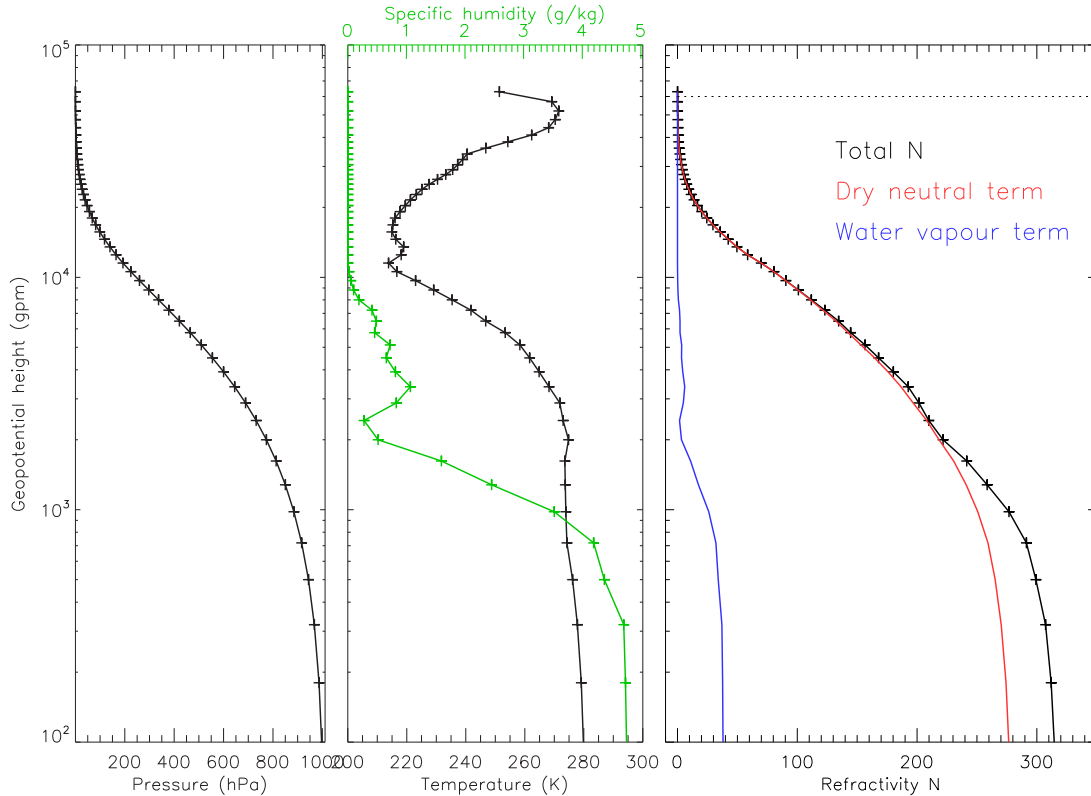


Figure 1.1: Contribution of the dry neutral atmosphere (term 1, Equation 1.1) and water vapour (term 2, Equation 1.1) to the refractivity profile computed for a sample atmosphere. Contributions from free electrons in the ionosphere and liquid water are too small to be shown.

therefore be used to relate refractivity to atmospheric pressure, temperature and humidity (6).

$$N = 77.6 \frac{p}{T} + 3.73 \times 10^5 \frac{e}{T^2} \quad (1.3)$$

The refractivity formula adopted by the International Union of Geodesy and Geophysics (IUGG) has been reviewed in recent years, given that accurate determination of refractivity is now critical for precise measurements by technology such as GPS. Research conducted over the last few decades was discussed by (5). A revised 3-term expression using best average coefficients from previous experiments relates refractivity to atmospheric parameters as

$$N = 77.6890 \frac{p}{T} + 3.75463 \times 10^5 \frac{e}{T^2} - 6.3938 \frac{e}{T} \quad (1.4)$$

The first coefficient in this expression was recomputed from an experimental coefficient of 77.6848 valid for a dry atmosphere with 300 ppm content of CO₂, to account for an increased carbon dioxide content of 375 ppm anticipated in 2004 (5). This expression is known to be applied in the operational data assimilation systems at Environment Canada (1) and Météo-France (P Poli, pers comm.) and is soon to be implemented in the operational assimilation system at the Met Office.

This document provides a summary of the sensitivity of refractivity calculations to the choice of refractivity formulation implemented in the ROPP software.

2 Results

2.1 Refractivity

Figure 2.1 illustrates the difference between refractivity values calculated using the formulations in Equations 1.3 (2-term) and 1.4 (3-term) for a range of different pressure and specific humidity values. The choice of refractivity formulation can lead to a difference of between 0.1 and 0.15% in N , with the 3-term equation (5) providing larger refractivity values than the 2-term equation (6). For a typical refractivity value in the upper troposphere of 300, this equates to a difference in N of about 0.3.

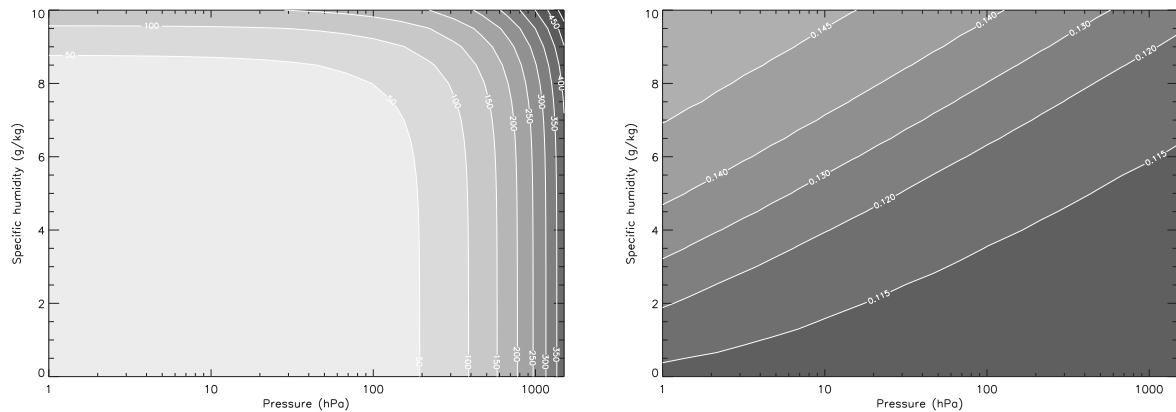


Figure 2.1: Sensitivity of the refractivity calculation to the formulation for refractivity. (a) Variation of refractivity with pressure p and specific humidity q (constant temperature 300 K). (b) Percentage difference between refractivity values computed using Equation 1.3 and Equation 1.4.

The impact of the refractivity formulation used in the ROPP forward model is illustrated in Figure 2.2 which shows the forward model refractivity computed for given model background atmospheric profiles, along with the percentage difference between results obtained using Equations 1.3 (2-term) and 1.4 (3-term). As anticipated from Figure 2.1 the largest sensitivity to the refractivity formulation occurs within the troposphere, where values of $N_2=320.282$ and $N_3=320.674$ are computed using Equations 1.3 and 1.4 respectively. The impact of using a different value for the first (dry neutral atmosphere) coefficient is evident above an altitude of 10^4 m where only the dry term contributes to the refractivity. In this region, the 3-term formula (Equation 1.4) computes values which are 0.115% greater than the 2-term formula.

The sensitivity of computed refractivity values in the forward model described here is of comparable magnitude to the sources of error in the observed refractivity values against which forward modelled values are compared (4), particularly in the troposphere. For example, (4) estimated that the percentage error in refractivity in the troposphere due to horizontal drift during an occultation is about 0.05% and the percentage error due to horizontal gradi-

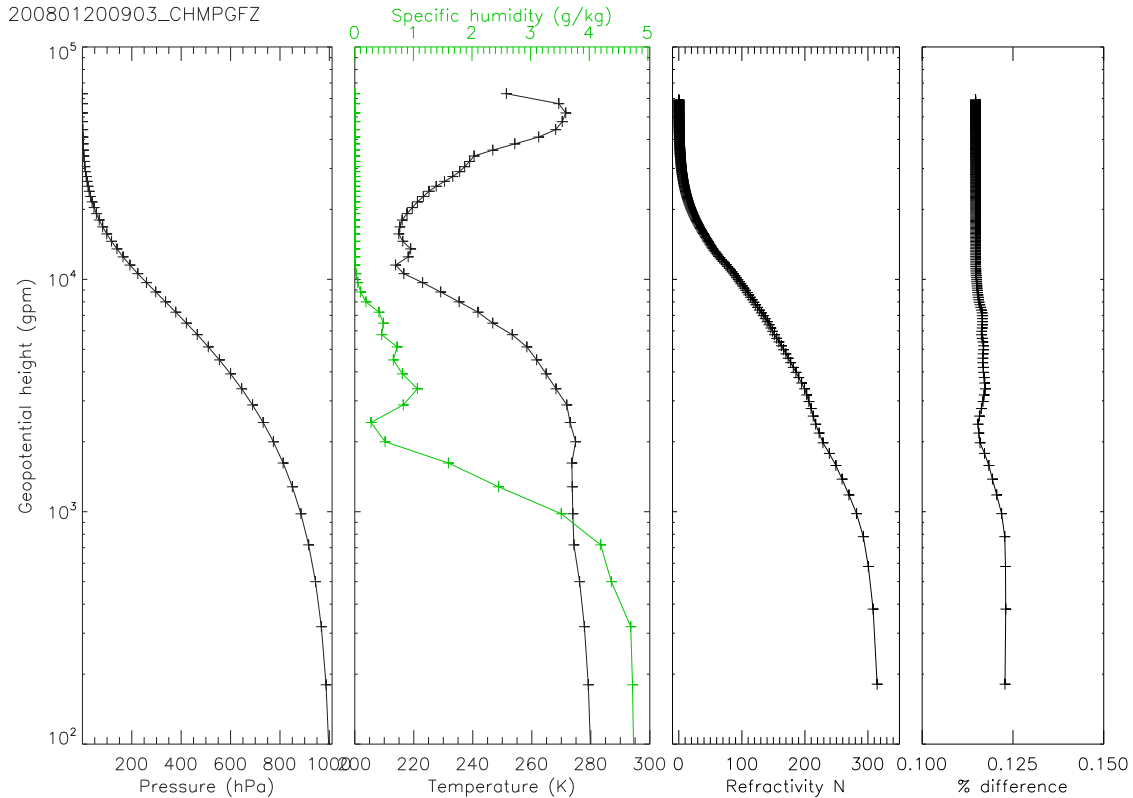


Figure 2.2: Sensitivity of the refractivity calculation to the formulation for refractivity for a given set of model background pressure, temperature and specific humidity profiles. The percentage difference profile shows the variation of $100(N_3 - N_2)/N_2$ as a function of height where N_2 is the refractivity computed using Equation 1.3 and N_3 is computed using Equation 1.4.

ents in the observed refractivity along the occultation track is about 0.2%.

2.2 Bending angle

The bending angle values computed in the ROPP forward model are derived from the refractivity profiles using the Abel transform. Figure 2.3 illustrates the sensitivity of bending angle values to the choice of refractivity formulation for the same atmospheric profiles in Figure 2.2. The impact of the refractivity formulation on bending angle values is more complicated than the impact on refractivity. At higher altitudes within the dry neutral atmosphere, the change of first coefficient again leads to a 0.115% difference in bending angle, preserving the differences in refractivity. At lower altitudes the cumulative impact of changes in refractivity values within the Abel transform leads to irregular changes in bending angle derived from the 2-term and 3-term expressions. In all cases, use of the 3-term refractivity formulation leads to larger bending angle values than the 2-term refractivity formulation. The maximum percentage difference for the case shown in Figure 2.3 is 0.31% at an altitude of 1181 m, corresponding to a difference in bending angle of 0.0046 degrees.

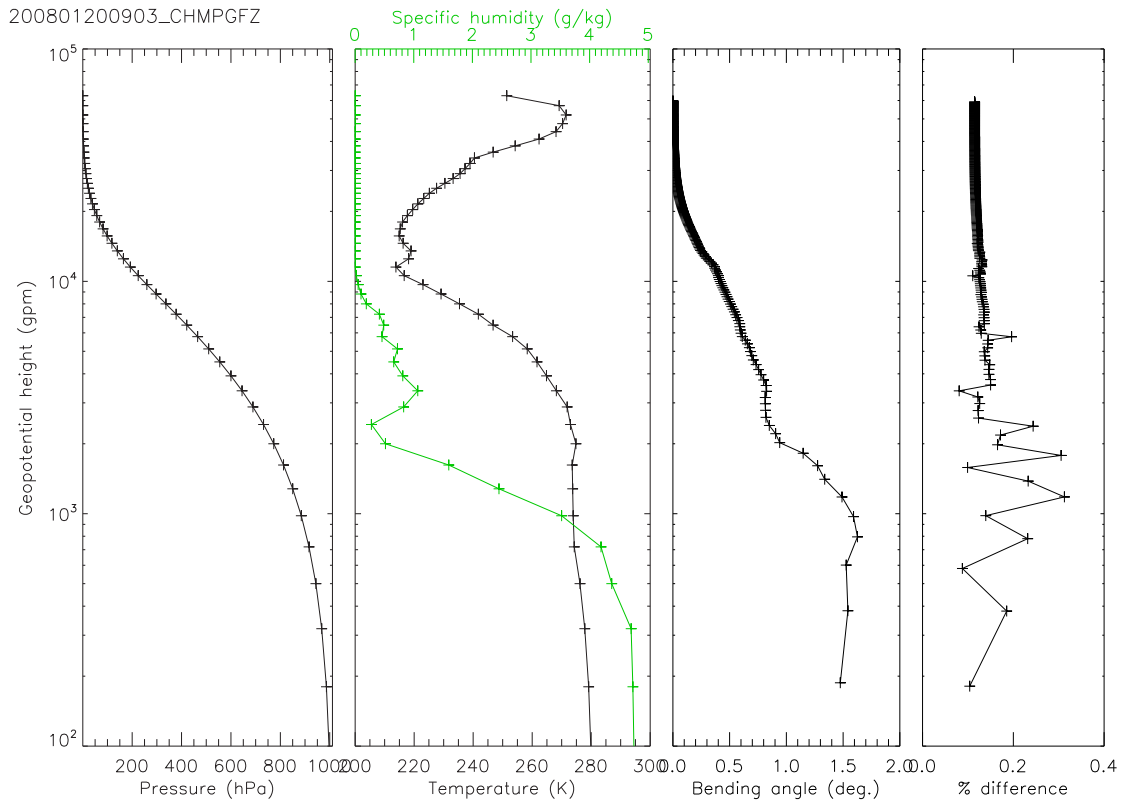


Figure 2.3: Sensitivity of bending angle values to the formulation for refractivity for a given set of model background pressure, temperature and specific humidity profiles. The percentage difference profile shows the variation of $100(\alpha_3 - \alpha_2)/\alpha_2$ as a function of height where α_2 is the bending angle derived from refractivity values computed using Equation 1.3 and α_3 is derived from refractivity values computed using Equation 1.4.

2.3 Summary

These tests indicate that the formulation used to compute refractivity from background atmospheric profiles has a small but not insignificant impact on the resulting refractivity and bending angle profiles. The sensitivity of these variables to the choice of refractivity formulation may be of comparable magnitude to other sources of error such as horizontal refractivity gradients along the ray during an occultation.

The 3-term refractivity formulation in Equation 1.4 is based on much research over the last few decades, attempts to account for changes in atmospheric composition over that time and is adopted by the International Association of Geodesy (5). It is therefore recommended that Equation 1.4, along with the corresponding tangent linear and adjoint codes, is implemented by users for GPSRO processing when provided in future releases of the ROPP software.

Bibliography

- [1] Aparicio, J. M. and Deblonde, G. (2008) Impact of the assimilation of CHAMP refractivity profiles on Environment Canada global forecasts. *Submitted to Monthly Weather Review*
- [2] Gultepe, I. and Isaac, G. A. (1997) Liquid Water Content and Temperature Relationship from Aircraft Observations and Its Applicability to GCMs *Journal of Climate* **10** 446-452.
- [3] Hajj, G.A. and Romans, L.J. (1998). Ionospheric electron density profiles obtained with the Global Positioning System: results from the GPS/MET experiment *Radio Sci.* **3** 157-190.
- [4] Kursinski, E. R., Hajj, G. A., Schofield, J. T., Linfield, R. P. and Hardy, K. R. (1997) Observing Earth's atmosphere with radio occultation measurements using the Global Positioning System. *J. Geophys. Research* **102** 23429-23465
- [5] Rüeger, J. M. (2002) Refractive index formulae for electronic distance measurement with radio and millimetre waves. Unisurv Report S-68. School of Surveying and Information Systems, University of New South Wales. [For a summary see http://www.fig.net/pub/fig_2002/Js28/JS28_rueger.pdf]
- [6] Smith, E. K. and Weintraub, S. (1953) The constants in the equation for atmospheric refractive index at radio frequencies. *Proc. IRE* **41** 1035-1037

GRAS SAF Reports

SAF/GRAS/METO/REP/GSR/001	Mono-dimensional thinning for GPS Radio Occultation
SAF/GRAS/METO/REP/GSR/002	Geodesy calculations in ROPP
SAF/GRAS/METO/REP/GSR/003	ROPP minimiser - minROPP
SAF/GRAS/METO/REP/GSR/004	Error function calculation in ROPP
SAF/GRAS/METO/REP/GSR/005	Refractivity calculations in ROPP
SAF/GRAS/METO/REP/GSR/006	Levenberg-Marquardt minimisation in ROPP
SAF/GRAS/METO/REP/GSR/007	Abel integral calculations in ROPP
SAF/GRAS/METO/REP/GSR/008	ROPP thinner algorithm
SAF/GRAS/METO/REP/GSR/009	Refractivity coefficients used in the assimilation of GPS radio occultation measurements
SAF/GRAS/METO/REP/GSR/010	Latitudinal Binning and Area-Weighted Averaging of Irregularly Distributed Radio Occultation Data
SAF/GRAS/METO/REP/GSR/011	ROPP 1dVar validation

GRAS SAF Reports are accessible via the GRAS SAF website <http://www.grassaf.org>.